Preparation of Adsorbent Based on Polyacrylate Latex Solid Waste and Its Application in the Treatment of Dye Wastewater

Weixu Sun,[#] Tao Liu,[#] Kai Xia, Jingye Zhou, Xin Liu,* and Xiaodong Zhang*

ACCESS | Metrics & More | Article Recommendations | SI Supporting Information

ABSTRACT: It is a great challenge to sustainably produce and apply water-based coatings and inks in terms of realizing the green resource utilization of polyacrylate latex solid waste (PLSW) and avoid its secondary pollution. In this paper, a kind of high value-added amphoteric ion-exchange resin (AIER) was prepared by using diethylenetriamine to amidate PLSW under the optimized conditions from a Box-Behnken design. Its adsorption and regeneration properties and the universality of the method were investigated. The results suggested that AIER possessed a high removal efficiency to anionic dyes, and the batch dye adsorption processes were endothermic and spontaneous, which is consistent with a pseudo-second-order kinetic model. The penetration adsorption capacities of AIER were recorded to be 987.08 mg/g for RR239 and 1037.75 mg/g for RB5 at the optimized operating conditions of column height = 6.4 cm, flow rate = 1 mL/min, and dye solution of 500 mg/L. They were more than 200 times larger than that of commercial activated carbon when the mixture composed of AIER particle and diatomite particle (filter aid agent) was used as a fixed-bed adsorbent. Zeta potential analysis results indicated that the good adsorption and regeneration performances of AIER were mainly attributed to the presence of amino and carboxyl groups in the molecular structure of AIER. Most importantly, this method possessed excellent practicability and universality for different types of PLSW from factory wastewater. The results provide a feasible method and theoretical basis for the green resource utilization of PLSW, and the goal of "waste control by waste" was fundamentally achieved.

1. INTRODUCTION

In recent years, with the continuous improvement of public environmental awareness, many countries and regions have formulated regulations to limit the emission of volatile organic compounds (VOCs).[1−7] The increasing emphasis on environmental protection is also driving the traditional oil-based paints and inks that generate a large amount of VOC to low-toxicity, no odor, noncorrosiveness, and flame-retardant water-based coatings and inks.[8,9] At present, the water-based coatings and inks based on polyacrylate latex resins have become the main product types, and they occupy a large share in the international market[10−14] and will continue to increase.[15]

However, a large amount of high-concentration wastewater containing polyacrylate copolymers is usually generated during the production and application of water-based coatings and inks.[16] The chemical composition of this kind of wastewater is quite complex, and the chemical oxygen demand (COD) is usually between 4000 and 18 000 mg/L, while the biochemical oxygen demand (BOD5) is usually between 1200 and 5000 mg/L, which is difficult to biodegrade.[17] Once it is discharged into the water body directly, it will not only cause environmental pollution but also destroy the ecological balance.

In the traditional treatment process of polyacrylate latex wastewater, a large number of solid pollutants in the wastewater are removed mainly by a pretreatment method of flocculation and filtration. Then the pretreated wastewater is chemically or biochemically treated to further reduce the COD of the wastewater, in accordance with the emission standards.[18] The main focus of the traditional process is on whether the treated wastewater can be reused or accord with the emission standards, while there are relatively few studies on the green resource utilization of the large amounts of polyacrylate latex solid waste (PLSW) generated during the treatment process. For this type of solid waste, one study has shown that its overall degradation rate in the soil is less than 1% every six months.[19] Studies have also shown that this kind of solid waste is not suitable for the preparation of activated carbon due to its low cross-linking degree (the dosage of cross-linking agent is usually 1−5 wt % of total monomer mass),[20−24] which can be attributed to the fact that, during the pyrolysis process, more than 90% of its weight will be converted to volatile substances with high VOC content and complex components (usually containing the N element).[25,26] As a result, the widely adopted

methods of disposing of PLSW by incineration or burial will inevitably cause secondary pollution and a large number of organic carbon sources and bring a heavy burden for enterprises and environment.[16] Therefore, how to realize the green resource utilization of PLSW and avoid its secondary pollution are great challenges to the sustainable production and application of water-based coatings and inks.

Amphoteric ion-exchange resins have received widespread attention due to their excellent performance in the fields of mixed element separation, chemical analysis, and wastewater treatment, especially in the treatment of anionic dye wastewater.[27−31] They have the characteristics of high adsorption and exchange capacity, easy regeneration with lye, and very low consumption of specific alkali.[32−34] They are usually subdivided into polystyrene-based polymer and polyacrylate-based polymer. Polyacrylate amphoteric ion-exchange resins are usually the ammoniated products of cross-linked acrylate copolymer precursors. Among them, the amino groups introduced by the amidation reaction work as the basic sites, while the carboxyl groups from the (meth)acrylic acid monomers usually work as the acidic sites.[35] Generally, the amount of cross-linking agent used in the preparation of the precursors exceeds 5 wt % for inhibiting its swelling property.[36]

From the perspective of structural classification, the solid wastes generated from the wastewater treatment process of polyacrylate latex for water-based coatings and inks are mainly divided into pure acrylate copolymer resins, styrene-acrylate copolymer resins, and vinyl acetate-acrylate copolymer resins.[37] Otherwise, in order to increase the stability of the emulsion, 1−10 wt % of (meth) acrylic monomer is usually added during the preparation of polyacrylate latex. The contents of the acrylic ester structural units in the molecular structure of pure acrylate copolymer resin and styrene-acrylate copolymer resin are usually greater than 50 wt %. They have the potential of preparing amphoteric ion-exchange resins (weak-base and weak-acid) through an amidation reaction with polyamine. The content of the acrylic ester structural units in the molecular structure of vinyl acetate-acrylate copolymer resin is usually less than 20 wt %,[38] which will most likely lead to a lower ion exchange capacity after amidation modification.

In addition, compared with polyamine polyacrylamide ion-exchange resin, polyacrylate latex resins used for water-based coatings and inks generally have a lower cross-linking degree; therefore, ion-exchange resins prepared by them usually have a high swelling degree.[39] It is well-known that an adsorbent with a higher swelling degree applied to a fixed-bed column will cause high column pressure and make the fixed-bed column unable to operate.[40−42] For this case, a filter aid is usually mixed into the adsorbent to solve the problem of high column pressure.

To avoid secondary pollution, the resource utilization method of PLSW was studied in this paper. By using diethylenetriamine (DETA) to amidate PLSW, an amphoteric ion-exchange resin (AIER) was prepared under the optimized amidation reaction conditions, and its static and dynamic adsorption (using diatomite particles as a filter aid agent) and regeneration properties were investigated. More importantly, the experimental results confirm that the method presented in this study has practicability and universality in treating PLSWs that come from different sources of wastewater that include polyacrylate latex for water-based coatings and inks.

2. EXPERIMENTAL SECTION

2.1. Reagent. The reagents, DETA, hydrochloric acid, and absolute ethanol were of analytically pure grade from Sinopharm Chemical Regent Co., Ltd. The diatomite was supplied by the Linqu Shanwang Chemical Company. Reactive red 239 (RR239), and reactive black 5 (RB5), from BASF, were purified according to a procedure from the literature,[43] and the molecular structures of the dyes were listed in Table S1.

2.2. PLSW. In order to quantify the structural composition of PLSW and facilitate the exploration of its influence on the experimental results, a polyacrylate latex from Rizhao Guangda Building Materials Co., Ltd. was adopted as the research object. It was prepared by an emulsion polymerization of 2.00 wt % of methacrylic acid, 3.43 wt % of methyl acrylate, 28.07 wt % of ethyl acrylate, 39.97 wt % of butyl acrylate, 26.17 wt % of styrene, and 1.36 wt % of N,N-methylene bis(acrylamide). The PLSW was extracted as follows: under stirring, 100 g of the above latex was acidified by 20 mL of HCl solution (2 mol/L) to compel the demulsification and precipitation of polyacrylate copolymer; after filtration, the filter cake was washed three times with 250 mL of deionized water and then washed three times with 250 mL of absolute ethanol to remove the emulgator. Then, the filter cake was dried at 110 °C to a constant weight, and the PLSW was obtained.

2.3. Preparation and Characterization of Amphoteric Ion-Exchange Resin. The ester group content of PLSW was measured by the method described in sections 6 and 7 of the Supporting Information. 200 g of the PLSW was added to a 1000 mL reaction kettle equipped with a stirrer, a thermometer, a reflux condenser, and a water separator. The reactor was heated to 140−180 °C with stirring. Then DETA was added dropwise according to the molar ratio of DETA/ester group content of PLSW (D/E). After the dripping was completed, the stirring was continued, and the reaction was maintained at a constant temperature for 6−10 h, while the mixed alcohol (mainly composed of methanol, ethanol and butanol) was recovered. The mixture was then cooled to room temperature. The product was added into 500 mL of deionized water, stirred at room temperature for 1 h, and filtered, and then the filter cake was washed with deionized water to neutrality. The filtrate was collected for recovering DETA through distillation, and the filter cake was added to 500 mL of a 0.1 M hydrochloric acid solution. After it was stirred at room temperature for 1 h, it was filtered (the filtrate could be recycled), and then the filter cake was dried, crushed, and sieved. The AIER (particle diameter in the range of 58−75 μm) was obtained.

To optimize the preparation process conditions of AIER, a Box-Behnken design of response surface methodology was applied according to the literature.[44,45] Thereinto, the amidation reaction temperature, time, and D/E molar ratio of AIER were set as the independent variables, and the adsorption capacity of AIER on RR239 was set as the dependent variable. The AIER was characterized by Fourier transform infrared (FT-IR) spectroscopy (Nicolet Is10, PerkinElmer Waltham), scanning electron microscopy (SEM) (JSM-7800F), element analyzer (Vario Macro Cube, Elementar), Zeta potentiometer (Malvern nano ZS, Beijing Oulan Technology Development Co., Ltd.), and Brunauer-Emmett-Teller (BET) (JW-BK100A, JWGB SCI&TECH). In addition, a particle size analyzer (Rise-2008) was adopted to evaluate

swelling properties by measuring the average particle sizes of AIER particles after the particles were dried and the ones after an ultrasonic expansion in deionized water or anhydrous ethanol for 2 min.

2.4. Static Adsorption Experiment of AIER on Reactive Dyes. The standard curves of RR239 and RB5 were determined by referring to the methods in the previous achievements of our research team,[43] and the results were shown in Table S2. Using the controlled variable method, each group of experiments fixed four of the five factors, namely, AIER dosage of 0.5 g/L, dye concentration of 500 mg/L, adsorption temperature of 20 °C, NaCl concentration of 0 g/L, and dye solution pH = 1, to examine the influence of the remaining factor (as the variate). In 100 mL of dye solution with a certain concentration and pH value, a certain amount of AIER and NaCl was added, and then the solution was oscillated at a set temperature for 24 h to reach the entire adsorption equilibrium. After this, 0.1 mL of dye solution was extracted through a needle filter for determining the dye solution concentration after adsorption by a UV−visible spectrophotometer combined with the standard curve, and then the dye adsorption capacity of AIER was calculated according to the literature.[43]

2.5. Adsorption Experiment of AIER on Reactive Dyes in a Fixed-Bed Column. The AIER had a certain swelling property due to its low cross-linking degree, which would cause excessive pressure in the AIER liquid−solid fixed-bed column. Therefore, it was necessary to adopt a porous and strong rigid material as a filler and mix it with the AIER to improve the liquid flow in the column. Cheap and readily available diatomite (75−106 μm) was selected and used as the filler, and the mixture of diatomite and AIER with a mass ratio of 3:2 (the minimum ratio when the hydraulic pressure on the advection pump showed zero) was used as a fixed-bed adsorbent for studying the dynamic adsorption of AIER. The penetration adsorption capacities of diatomite to RR239 and RR5 were determined to be 0.62 and 0.47 mg/g, respectively, and the penetration adsorption capacity of AIER was the penetration adsorption capacity of the mixed adsorbent minus the penetration adsorption capacity of diatomite. Here, the penetration adsorption capacity was referred to the maximum adsorption capacity of the adsorbent when the effluent of the fixed bed did not contain dyes. The adsorption device was shown in Figure 1, in which the height of the column was 20 cm, the inner diameter was 1.2 cm, and there was an adjustable piston inside.

2.6. Reusability of AIER. The reusability of the column was evaluated by five successive desorption-adsorption cycles. The used AIER was regenerated by passing the desorbing agent NaOH solution (0.1 mol/L) through the column with the constant flow rate of 0.1 mL/min. After desorption, the

column was washed with distilled water until the effluent was nearly neutral.

2.7. Practicability and Universality Study. To verify the practicability and universality of the method, nine kinds of production wastewater of polyacrylate lattices for different uses were collected. According to the above method, PLSWs were extracted, and their ester contents were analyzed, respectively, then each PLSW was aminated with DETA under the optimized conditions. The weak acid group exchange capacity (EC_a) and weak base exchange capacity (EC_b) of the prepared amphoteric ion-exchange resins were determined according to the method of GB/T 19861−2005, and their penetration adsorption capacities were determined according to the method described in section 2.5.

3. RESULTS AND DISCUSSION

3.1. Preparation and Characterization of AIER. A Box-Behnken design of the response surface methodology was adopted to reveal the influences of amidation reaction temperature, reaction time, and D/E ratio of PLSWs on the adsorption capacity of AIER. The results are shown in Tables S3 & S4, equation S9, and Figure 2. From the data including the p-value, lack of fit, R^2, $AdjR^2$, $PredR^2$, and Adeq Precision, it could be concluded that the fitting equation was applicable and had enough signal. The results indicated that the resulting equation (Box-Behnken design) could well be used to predict the practical performance of the AIER. A temperature of ~165.23 °C, a time of 8.20 h, and a D/E ratio of 1.46 were found to be the optimum conditions, and the predicted adsorption capacity was 627.27 mg/g. These results were validated by a control experiment under the predicted optimum conditions, and the adsorption capacity of the prepared AIER was 625.14 mg/g, which was basically consistent with the predicted value.

It was demonstrated that the adsorption capacities of AIER all passed through a maximum as a function both of the reaction temperature and the reaction time, and then their variation trends leveled off and decreased at higher temperatures and longer times because of amide group decomposition.[46] With the increase of the D/E ratio, the adsorption capacity of the AIER showed a tendency to increase rapidly and then stabilize. The inflection points appeared in a D/E ratio of 1.46.

Figure 3a shows FT-IR spectra of PLSW and AIER. It was found that AIER had amide group N−H and C=O characteristic absorption peaks at 3270 and 1640 cm^{-1}, respectively, and both of them were obviously increased with the significant weakening of the ester characteristic peak of PLSW at 1730 cm^{-1}. This indicated that the amidation reaction had occurred between DETA and PLSW. Also, it could be seen that both PLSW and AIER contained the O−H stretching vibration peak of a carboxyl group at 3410 cm^{-1}. These results indicated that AIER had the structural characteristics of an amphoteric ion-exchange resin.

As can be seen from the SEM images of PLSW and AIER in Figure 3b, the surface of PLSW was smooth and compact, whereas the surface of AIER was rough, irregular, and loose, indicating that the particle surface morphology of the product AIER was obviously different from that of original material PLSW after the amidation reaction. In summary, the schematic diagram of the amidation reaction between PLSW and DETA was shown in Figure 3c.
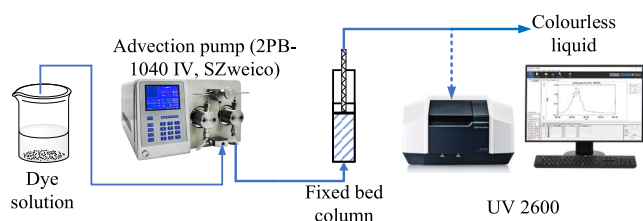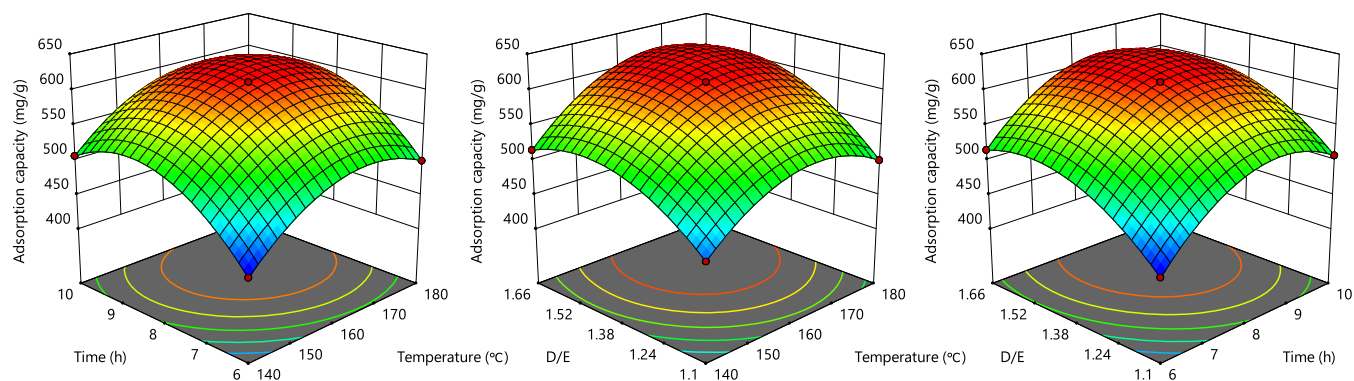

Figure 1. Diagram of dynamic adsorption experiment.

Figure 2. Optimization of the absorption capacity of AIER on RR239 at different operating conditions.
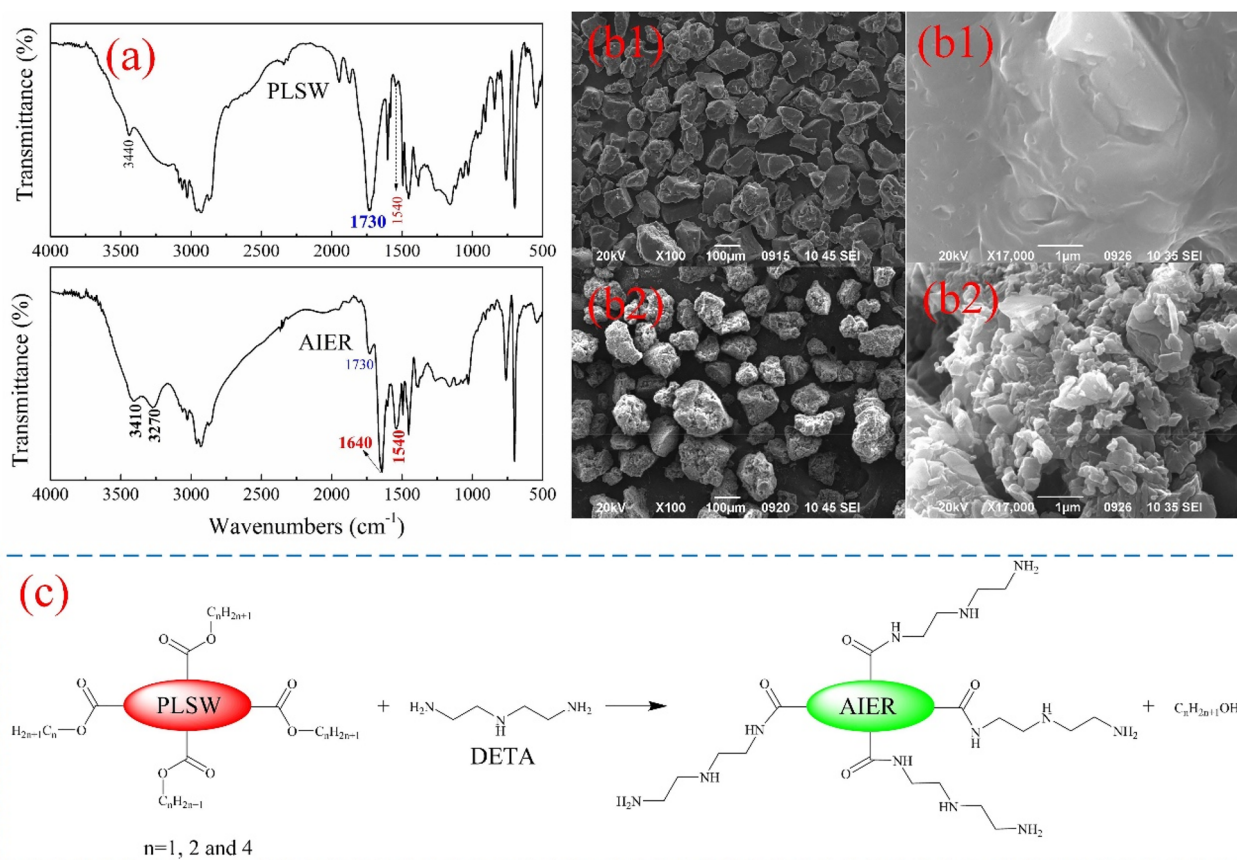

Figure 3. (a) FT-IR spectra of PLSW and AIER, (b1) SEM images spectra of PLSW, (b2) SEM images spectra of AIER, (c) schematic diagram of the amidation reaction between PLSW and DETA.

Table 1. Basic Physical Properties of PLSW and AIER[a]

	elemental analysis (wt %)				average particle size (μm)		
sample	C	H	N	S (m^2/g)	raw	water	absolute ethanol
PLSW	76.02	8.80	0.27	3.14	NA	NA	NA
AIER	54.30	9.87	9.77	1.71	58−75	416.57	116.81

[a]NA indicates not applicable.

Table 1 shows the elemental analysis, specific surface area, and swelling property results of PLSW and AIER. The N content of AIER was much higher than that of PLSW, which further proved that the amidation reaction had occurred between DETA and PLSW. The specific surface area of PLSW and AIER were both less than 5 m²/g. Therefore, the higher adsorption capacity of AIER was not entirely dependent on its

specific surface. AIER had a large swelling degree in water. Once it was directly used as a fixed-bed column adsorbent, it might cause excessive column pressure due to swelling.

3.2. Batch Adsorption Experiments. The dye removal percentages are presented in Figure 4 as functions of the dosage of AIER, concentration of dye, adsorption temperature, concentration of NaCl, and solution pH value. It was found
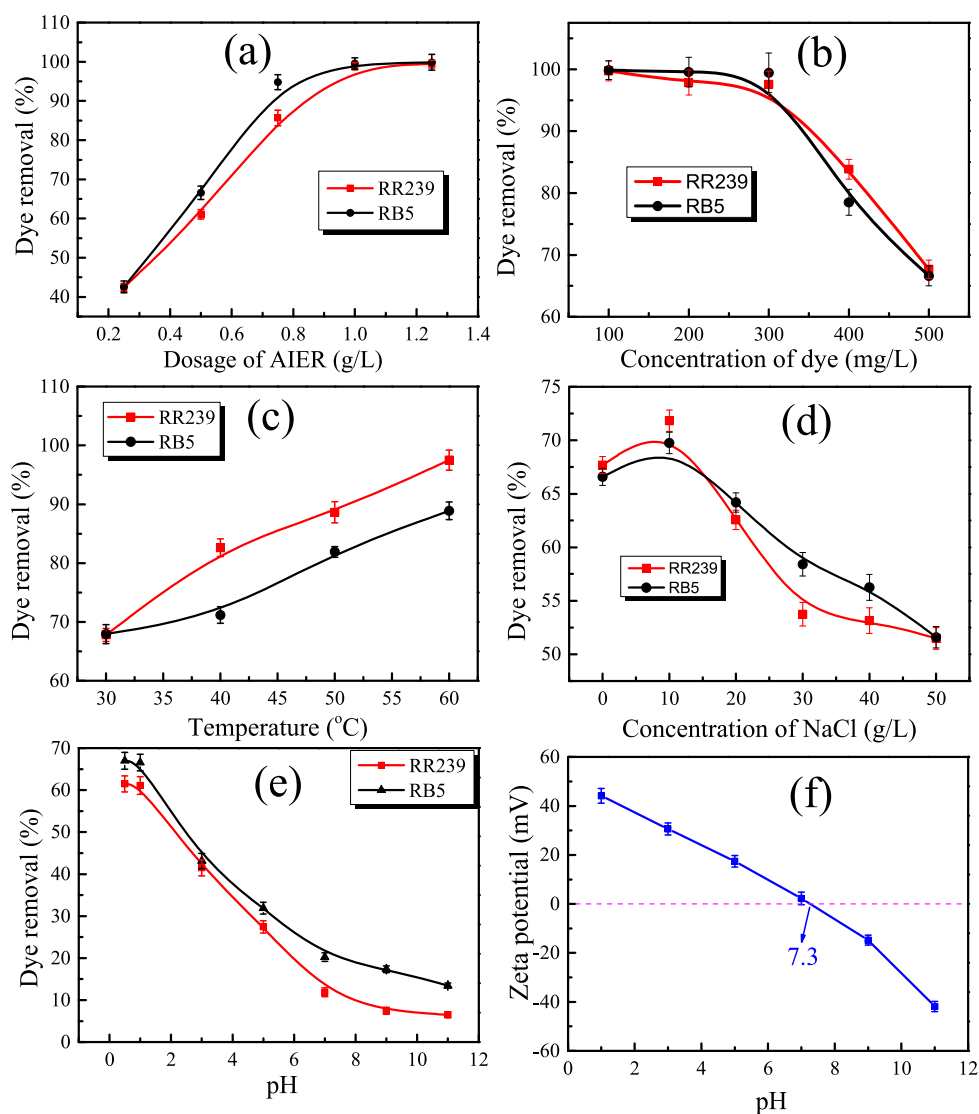
Figure 4. Influence of the adsorption conditions on the dye removal efficiency of AIER. Experimental operating conditions: (a) dye concentration of 500 mg/L, adsorption temperature of 20 °C, NaCl concentration of 0 g/L, and dye solution pH = 1, (b) AIER dosage of 0.5 g/L, adsorption temperature of 20 °C, NaCl concentration of 0 g/L, and dye solution pH = 1, (c) AIER dosage of 0.5 g/L, dye concentration of 500 mg/L, NaCl concentration of 0 g/L, and dye solution pH = 1, (d) AIER dosage of 0.5 g/L, dye concentration of 500 mg/L, adsorption temperature of 20 °C, and dye solution pH = 1, (e) AIER dosage of 0.5 g/L, dye concentration of 500 mg/L, adsorption temperature of 20 °C, and NaCl concentration of 0 g/L. The Zeta potential of AIER (f).

that increasing the dosage of AIER and temperature, lowering the dye concentration and the dye solution pH, and adding an appropriate amount of inorganic salt (NaCl) could promote the decolorization of the dye solutions by AIER.

A decrease of the dye solution pH from ∼7 to 0.5 resulted in rapid increases in the decolorization efficiency of AIER. The Zeta potential analysis was used to determine the influence of pH on adsorption [Figure 4f]. AIER possessed a positive charge on the surface in the pH range of 0.5−7.3, which was attributed to the amino groups. With the increase of the pH, the Zeta potential values of AIER gradually decreased, which meant that the electrostatic interactions between the adsorbent and dye molecules correspondingly weakened, resulting in lower dye removal percentages at higher pH values. Under alkaline conditions, the hydroxide ions in solution could compete with dye molecules to combine with AIER. Meanwhile, the carboxyl groups of AIER were transformed into carboxylate ions, which increased the repulsive force

between the AIER and the dye molecules. In addition, abundant carboxyl groups also provided potential for AIER to desorb anionic dyes.

The real dye wastewater usually contains a number of inorganic salts,[47] which will affect the adsorption performance of adsorbents. When the concentration of inorganic salts is low, its anions can promote the movement of anionic dye molecules to the surface of the adsorbent, thus increasing the adsorption capacity of the adsorbent. When the concentration of inorganic salts is high, its anions will compete with the anionic dyes for the adsorption position on the surface of the adsorbent, resulting in a decrease in the adsorption capacity of the adsorbent.

3.3. Thermodynamics, Kinetics, and Isotherm Analyses. Table 2 shows the thermodynamic characteristics of the adsorption processes. The $\Delta H°$ and $\Delta G°$ values were found to be positive and negative, respectively, indicating that dye adsorption processes might be endothermic and sponta-

Table 2. Thermodynamic Parameters of the Adsorption Process

dye	$\Delta H°$ (kJ·mol^{-1})	$\Delta S°$ (J·mol^{-1}·K^{-1})	$\Delta G°$ (kJ·mol^{-1}) 303 K	313 K	323 K	333 K
RR239	77.25	89.30	−21.02	−23.84	−25.93	−31.02
RB5	38.25	83.14	−21.04	−22.13	−24.27	−26.80

neous.[48] The enhanced randomness and disorder in the system were evidenced by positive $\Delta S°$ values.

Figure 5a,b provides a comparison of the two batch adsorption kinetics models. The acquired data were found to be more compatible with the pseudo-second-order model for both reactive dyes, with correlation coefficient values of more than 0.99 for both (see Table 3). The pseudo-second-order kinetic model might describe the batch adsorption process of AIER to reactive dyes, according to the fitting findings, and the adsorption process was mainly one of chemical adsorption.

The dye adsorption isotherm plots and isotherm parameters of AIER dye adsorption are given in Figure 5c,d and Table 4, respectively. The experimental results of AIER adsorption to two reactive dyes were both better fitting to the Langmuir model ($R^2 > 0.99$), which revealed that they were monolayer adsorption processes. It was consistent with the characteristics of electrostatic adsorption.

According to a Zeta potential analysis and regeneration test, the probable mechanisms of the interactions between AIER and reactive dyes were proposed and illustrated in Figure 6. AIER possessed the positive potential within the solution pH ranging from 0.5 to 7.3 (see Figure 4), while the reactive dyes

Table 3. Parameters of Three Dye Kinetic Models for CB Adsorption

model	parameters	RR239	RB5
pseudo-first-order kinetic	$q_{e, fac}$ (mg·g^{-1})	611.04	665.92
	$q_{e, the}$ (mg·g^{-1})	589.94	644.19
	k_1 (min^{-1})	0.004	0.003
	R^2	0.970	0.966
pseudo-second-order kinetic	$q_{e, fac}$ (mg·g^{-1})	611.04	665.92
	$q_{e, the}$ (mg·g^{-1})	645.16	705.29
	k_2 (10^{-6} g·mg^{-1}·min^{-1})	8.80	7.61
	R^2	0.993	0.991

Table 4. Parameters of Langmuir Model and Freundlich Model

dye	Langmuir model Q_0 (mg/g)	K_L (10^{-2} L/mg)	R^2	Freundlich model K_F	n	R^2
RR239	684.932	0.616	0.999	295.645	2.016	0.831
RB5	696.670	0.999	0.998	1.148	7.246	0.593

contained multiple $-SO_3^-$ groups within their molecular structures (see Table S1) and possessed negative charges in an aqueous solution. This meant that there should be strong electrostatic interactions between AIER and the reactive dyes, which was also the main adsorption mechanism for AIER-adsorbing reactive dyes.

3.4. Fixed-Bed Adsorption Experiments. Figure 7 shows the penetration curves of reactive dye solutions treated
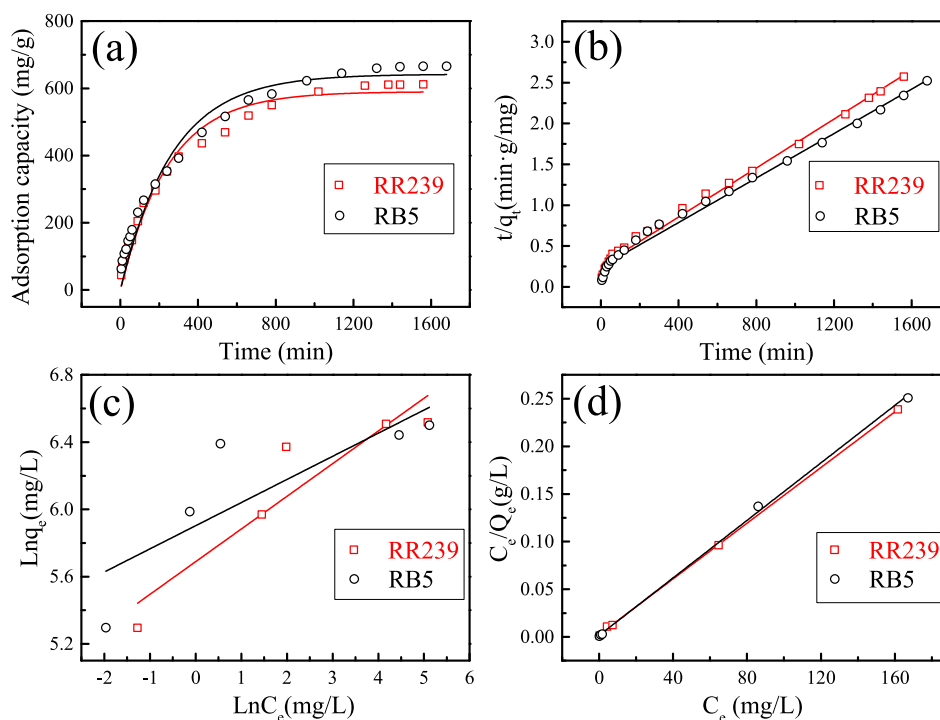

Figure 5. Kinetics and isotherms of the batch adsorption process of AIER, (a) pseudo-first-order kinetic (AIER dosage of 0.5 g/L, dye concentration of 500 mg/L, adsorption temperature of 20 °C, NaCl concentration of 0 g/L, and dye solution pH = 1), (b) pseudo-second-order kinetic (AIER dosage of 0.5 g/L, dye concentration of 500 mg/L, adsorption temperature of 20 °C, NaCl concentration of 0 g/L, and dye solution pH = 1), (c) Freundlich isotherm (AIER dosage of 0.5 g/L, adsorption temperature of 20 °C, NaCl concentration of 0 g/L, and dye solution pH = 1), (d) Langmuir isotherm (AIER dosage of 0.5 g/L, adsorption temperature of 20 °C, NaCl concentration of 0 g/L, and dye solution pH = 1). The solid lines were the corresponding regressions.
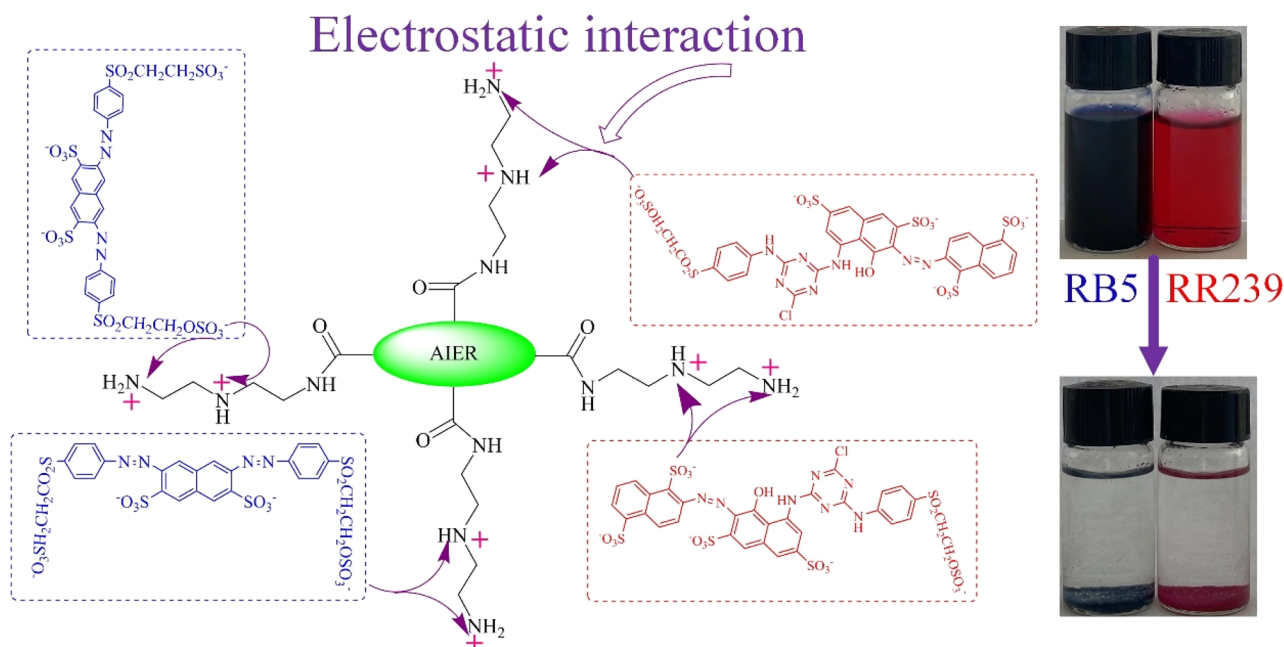
Figure 6. Schematic diagram of AIER adsorption mechanism on an anionic dye.

by the column. The parameters of each penetration curve are shown in Tables S5−S7. The breakthrough point of the fixed-bed column in this research is defined as the point at which the dye concentration of the effluent reached above zero. From Figure 7, it could be found that the penetration adsorption capacities of AIER were recorded to be 987.08 mg/g for RR239 and 1037.75 mg/g for RB5 at the experimental operating conditions of column height = 6.4 cm, flow rate = 1 mL/min, and dye solution of 500 mg/L, respectively. The empty bed contact time (EBCT) of the adsorption column corresponding to the above operating conditions was 7.22 min. This result indicated that the penetration adsorption capacities of AIER were at least 200 times larger than that of commercial activated carbon under the same conditions.[43]

The influences of the column height, initial dye concentration, and flow rate on the dye column adsorption process of AIER were investigated, and the corresponding penetration curves are shown in Figure 7. From Table S5, increasing the column height was beneficial to improve the penetration adsorption capacity of AIER. As seen from Figure 7c,d, the penetration curves became sharper, and the breakthrough time became shorter when the flow rate was increased from 1 to 1.5 mL/min. The adsorption performance of the fixed-bed column was enhanced at a lower flow rate. The reason is that the residence time of the dye molecules in the fixed-bed column could be reduced at a higher flow rate, and the dye molecules left the fixed-bed column before the establishment of an adsorption equilibrium.[49] From Figure 7e,f, the breakthrough time became longer with the initial influent concentrations decreased, which indicated that the ability of AIER to obtain a colorless effluent in the fixed-bed column could be enhanced at lower initial influent concentration. This phenomenon could be due to the driving force in the mass transfer process being stronger at higher concentration, and more dye molecules could result in more quickly saturating the column, and some molecules would be left unadsorbed.[50] This observation was similar to the report in a previous study.[43]

3.5. The Reusability of AIER. Figure 8 shows the regeneration times of the AIER-diatomite column and its regeneration efficiency. It can be seen from Figure 8 that, after five times of adsorption and four times of desorption on the fixed bed, the penetration adsorption capacity of the AIER-diatomite column for RR239 could be maintained above 90%, and the adsorption capacity for RB5 could reach 85%. In addition, the regeneration of the adsorption column could be achieved by consuming 160−200 mL of NaOH (0.1 mol/L) solution and ∼200 mL of deionized water. The dyes in highly concentrated dye wastewater produced after desorption can be recycled for other purposes through acidification and filtration, and a small amount of produced acid filtrate can be put into dye wastewater for readsorption treatment, so as to avoid effluent discharge.

It could be concluded that AIER had the ideal adsorption and regeneration capacity. A positive charge was attached to AIER by amino groups in an acidic condition.[51] On the one hand, it would generate electrostatic attraction with the negatively charged sulfonic acid group of the anionic dye, so that AIER could adsorb a large amount of anionic dye. On the other hand, an alkaline condition would convert the carboxyl groups of AIER into negatively charged carboxylate ions, which would repulsively react with the sulfonic acid groups of the adsorbed anionic dyes, making AIER have excellent recycling performance.[52]

3.6. Practicability and Universality Study. Nine kinds of PLSW were extracted from nine kinds of industrial wastewater of latex used for water-based coatings or inks. According to their ester group content (see Table S8), each PLSW was aminated with DETA under the optimized conditions shown in section 3.1. Their penetration adsorption capacities were evaluated under the optimized conditions shown in section 3.3, and the results were exhibited in Table 5. Combined with the data in Table S8, it could be concluded that the EC_b value and adsorption capacity of AIERs were positively correlated with the acrylate ester group content in the corresponding PLSW. The penetration adsorption
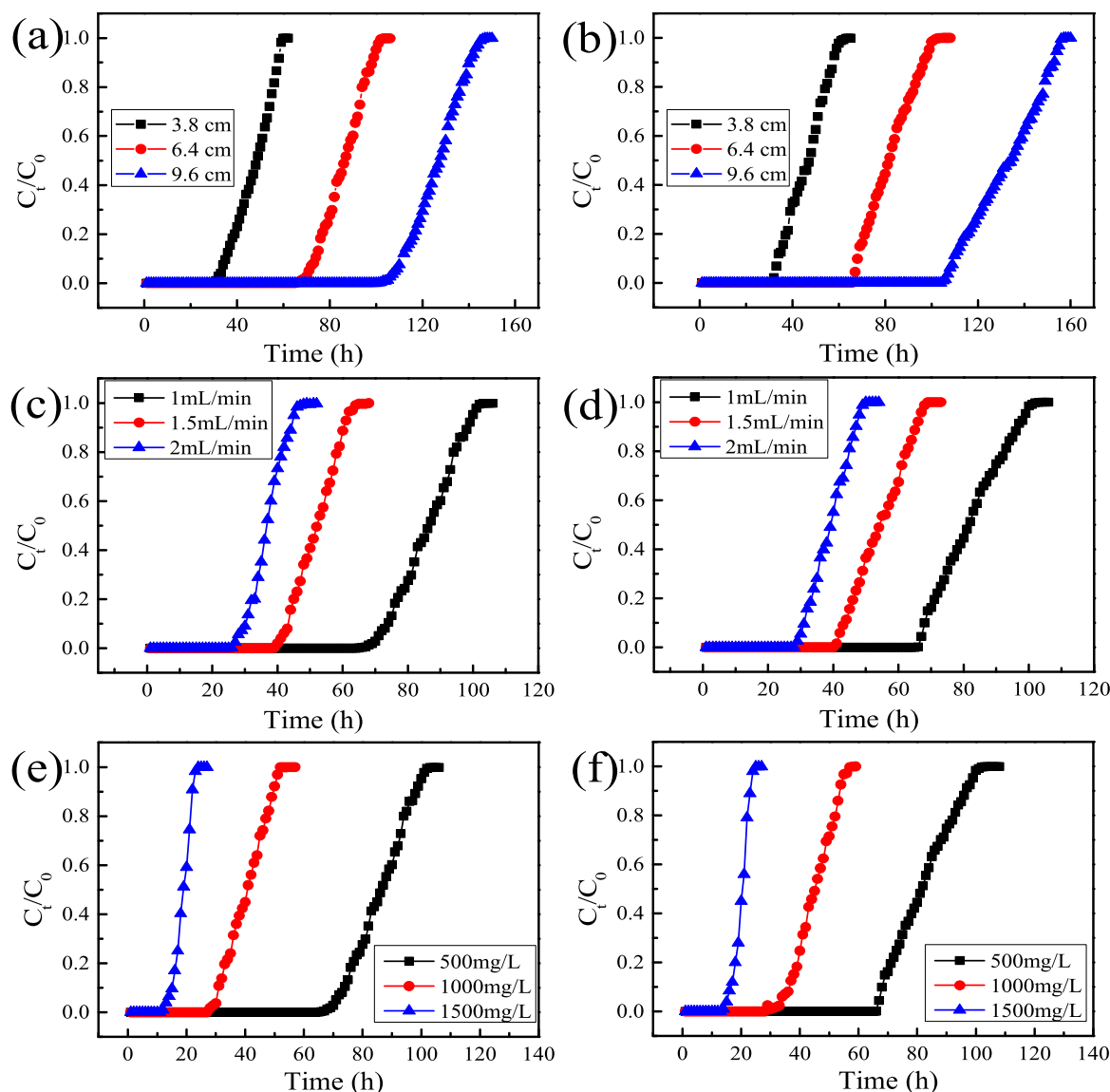
Figure 7. Breakthrough curves for dye adsorption in a fixed-bed column. Experimental operating conditions: (a) RR239 solution (500 mg/L), flow rate = 1 mL/min, (b) RB5 solution (500 mg/L), flow rate = 1 mL/min, (c) column height of 6.4 cm, RR239 solution (500 mg/L), (d) column height = 6.4 cm, RB5 solution (500 mg/L), (e) column height = 6.4 cm, flow rate = 1 mL/min, RR239 solution, (f) column height = 6.4 cm, flow rate = 1 mL/min, RB5 solution.
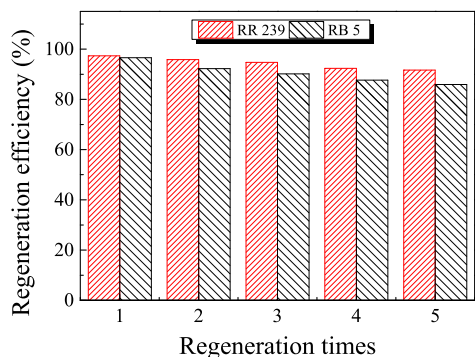

Figure 8. Reusability study of the AIER-diatomite column for adsorption of RR239 and RB5.

capacities of AIERs prepared from styrene-acrylate copolymer resins, pure polyacrylate copolymer resins, and vinyl acetate-acrylate copolymer resins were between 423.16 and 987.08 mg/g, 905.68−999.90 mg/g, and 184.57−352.16 mg/g, which were at least 80 times, 180 times, and 30 times more than that of commercial activated carbon (AC, methylene blue value of 150 mg/g), respectively, and all were close to or even surpassing that of the adsorbents with excellent adsorption performance reported in the literature.[43,53,54] However, when vinyl acetate acrylate copolymer resin reacts with DETA, the ester group of the acetate in the structure also participates in the amidation reaction, which will lead to a sharp increase in DETA consumption and high cost. Therefore, it is suggested to adopt other methods to modify the vinyl acetate-acrylate copolymer resin to improve its utilization value. In spite of this, the method explored in this paper was still practical and universal in green resource utilization of various PLSWs.

4. CONCLUSIONS

In order to avoid secondary pollution and realize the green resource utilization, PLSW was modified to AIER by amidation

Table 5. Comparison of the Adsorption Capacities of Various Adsorbents to RR239 and RB5[a]

classification	adsorbent	EC_a (mmol/g)	EC_b (mmol/g)	diatomite/AIER mass ratio	adsorption capacity (mg/g) RR239	RB5
activated carbon	AC	NA	NA	NA	4.81	4.92
styrene-acrylate copolymer resin	AIER	0.26	5.89	3:2	987.08	1037.75
	AIER-1	0.26	3.18	3:2	423.16	486.91
	AIER-2	0.31	4.06	3:2	613.48	696.47
	AIER-3	0.47	6.81	3:2	867.35	896.42
pure polyacrylate copolymer resin	AIER-4	0.30	7.41	3:2	905.68	1009.42
	AIER-5	0.94	7.92	3:2	954.18	1067.49
	AIER-6	0.35	8.02	3:2	999.90	1220.30
vinyl acetate-acrylate copolymer resin	AIER-7	0.08	1.12	7:4	184.57	208.24
	AIER-8	0.11	1.96	7:4	321.41	352.15
	AIER-9	0.10	2.35	7:4	352.16	384.67
cationic diatomite[43]	CD	NA	NA	NA	204.20	216.60
bone char[53]	BC	NA	NA	NA	NA	160.00
modified chitosan nanoparticles[54]	MCN	NA	NA	NA	200.00	NA

[a]NA indicates not applicable.

with DETA under the optimized conditions from a Box-Behnken design. The adsorption properties and regeneration properties of the AIER and the universality of the method were investigated. The results showed that the batch anionic dye adsorption processes of AIER were spontaneous, fast, and influenced by the dosage of adsorbent, the concentration of dye, the temperature, concentration of NaCl, and solution pH value, respectively. The column-penetrating adsorption capacities of AIERs were much larger than that of AC and adsorbents reported and still possessed high sorption performance to anionic dyes after five cycles of adsorption−desorption operations in column, indicating that the prepared AIER was a potential low-cost adsorbent in a fixed bed as an alternative to AC for treating anionic dye wastewaters. Most importantly, the method had excellent practicability and universality for high value-added reuse of PLSW extracted from polyacrylate latex wastewater, especially, from pure acrylate latex and styrene-acrylate latex wastewater produced in the process of factory production. In summary, a universal, sustainable, and high value-added resource utilization method of PLSW was presented in this research for the first time, and this method could provide a viable solution for waste control by waste.

■ ASSOCIATED CONTENT

Ⓢ Supporting Information

The Supporting Information is available free of charge at https://pubs.acs.org/doi/10.1021/acsomega.2c00690.

> Molecular structure of the dyes used in this study; standard curves of the reactive dyes; characterization tests; batch analysis of dye adsorption; fixed-bed column studies; determination of carboxyl group content in PLSW; determination of ester group content in PLSW; Box-Behnken design and experimental results for the response variable; significance test result of adsorption capacity response surface model; fitting equation of the relationship between amidation reaction conditions and adsorption capacities of AIER; parameters of column height on breakthrough curve; parameters of dye concentration on breakthrough curve; parameters of dye flow rate on penetration curve; application of the latex and eater group content of various PLSW (PDF)

■ AUTHOR INFORMATION

Corresponding Authors

Xin Liu − *College of Chemistry and Chemical Engineering, Qingdao University, Qingdao 266071, China*; Email: liuxinqdu@126.com

Xiaodong Zhang − *College of Chemistry and Chemical Engineering, Qingdao University, Qingdao 266071, China*; ⊙ orcid.org/0000-0002-3809-8838; Email: zhangxdqd@hotmail.com

Authors

Weixu Sun − *College of Chemistry and Chemical Engineering, Qingdao University, Qingdao 266071, China*

Tao Liu − *College of Chemistry and Chemical Engineering, Qingdao University, Qingdao 266071, China*

Kai Xia − *College of Chemistry and Chemical Engineering, Qingdao University, Qingdao 266071, China*

Jingye Zhou − *College of Chemistry and Chemical Engineering, Qingdao University, Qingdao 266071, China*

Complete contact information is available at: https://pubs.acs.org/10.1021/acsomega.2c00690

Author Contributions

[#]These authors contributed equally as the first author.

Notes

The authors declare no competing financial interest.

■ ACKNOWLEDGMENTS

■ REFERENCES

(1) Pelaez, M.; Nolan, N. T.; Pillai, S. C.; Seery, M. K.; Falaras, P.; Kontos, A. G.; Dunlop, P. S. M.; Hamilton, J. W. J.; Byrne, J. A.; O'Shea, K.; Entezari, M. H.; Dionysiou, D. D. A review on the visible

light active titanium dioxide photocatalysts for environmental applications. *Appl. Catal., B* **2012**, *125*, 331−349.

(2) Tibrewal, K.; Venkataraman, C. Climate co-benefits of air quality and clean energy policy in India. *Nat. Sustain.* **2021**, *4* (4), 305−313.

(3) Li, H. Y.; Zhao, S. N.; Zang, S. Q.; Li, J. Functional metal-organic frameworks as effective sensors of gases and volatile compounds. *Chem. Soc. Rev.* **2020**, *49* (17), 6364−6401.

(4) Yang, C.; Miao, G.; Pi, Y.; Xia, Q.; Wu, J.; Li, Z.; Xiao, J. Abatement of various types of VOCs by adsorption/catalytic oxidation: A review. *Chem. Eng. J.* **2019**, *370*, 1128−1153.

(5) Li, X.; Zhang, L.; Yang, Z.; Wang, P.; Yan, Y.; Ran, J. Adsorption materials for volatile organic compounds (VOCs) and the key factors for VOCs adsorption process: A review. *Sep. Purif. Technol.* **2020**, *235*, 116213.

(6) Parvaresh, V.; Hashemi, H.; Khodabakhshi, A.; Sedehi, M. Removal of dye from synthetic textile wastewater using agricultural wastes and determination of adsorption isotherm. *Desalination Water Treat.* **2018**, *111*, 345−350.

(7) Mirnasab, M. A.; Hashemi, H.; Samaei, M. R.; Azhdarpoor, A. Advanced removal of water NOM by Pre-ozonation, Enhanced coagulation and Bio-augmented Granular Activated Carbon. *Int. J. Environ. Sci. Technol. (Tehran)* **2021**, *18* (10), 3143−3152.

(8) Ho, J.; Mudraboyina, B.; Spence-Elder, C.; Resendes, R.; Cunningham, M. F.; Jessop, P. G. Water-borne coatings that share the mechanism of action of oil-based coatings. *Green Chem.* **2018**, *20* (8), 1899−1905.

(9) Nechyporchuk, O.; Yu, J.; Nierstrasz, V. A.; Bordes, R. Cellulose Nanofibril-Based Coatings of Woven Cotton Fabrics for Improved Inkjet Printing with a Potential in E-Textile Manufacturing. *ACS Sustain. Chem. Eng.* **2017**, *5* (6), 4793−4801.

(10) Green Coatings Market - Global Industry Analysis. https://www.zionmarketresearch.com/report/green-coatings-market (Published Date: December 11, 2020).

(11) Printing Inks Market - Global Industry Analysis. https://www.zionmarketresearch.com/report/printing-inks-market (Published Date: September 29, 2021).

(12) Zhou, C. E.; Zhang, Q.; Kan, C. W. Rheological properties of thickener for preparing digital printing ink for nylon carpets. *Fibers Polym.* **2016**, *17* (9), 1475−1479.

(13) Yu, S.; Du, Y.; Chen, Y.; Zhang, X.; Li, X.; Wang, H. Study on ethanol resistance stability and adhesion properties of polyacrylate latex for PE or BOPP film inks. *J. Appl. Polym. Sci.* **2022**, *139* (13), 51857.

(14) Lin, N.; Ye, Y.; Guo, Q.; Yu, J.; Guo, T. Effect of using ink containing polyacrylate and silicone surfactant on the inkjet printing of quantum dot films. *J. Inf. Dispersion* **2020**, *21* (2), 113−121.

(15) Gao, G.; Luo, G.; Xu, M.; Shouping, X.; Pi, P.; Wen, X. Synthesis and characterization of multiple-crosslinkable polyacrylate emulsion for PVC film ink. *Prog. Org. Coat.* **2020**, *138*, 105190.

(16) Zhao, X.; Ma, J.; Ma, H.; Gao, D.; Sun, Y.; Guo, C. Removal of polyacrylate in aqueous solution by activated sludge: Characteristics and mechanisms. *J. Clean. Prod.* **2018**, *178*, 59−66.

(17) Saitoh, T.; Yamaguchi, M.; Hiraide, M. Surfactant-coated aluminum hydroxide for the rapid removal and biodegradation of hydrophobic organic pollutants in water. *Water Res.* **2011**, *45* (4), 1879−1889.

(18) Song, Q.; Sun, Z.; Chang, Y.; Zhang, W.; Lv, Y.; Wang, J.; Sun, F.; Ma, Y.; Li, Y.; Wang, F.; Chen, X. Efficient degradation of polyacrylate containing wastewater by combined anaerobic-aerobic fluidized bed bioreactors. *Bioresour. Technol.* **2021**, *332*, 125108.

(19) Wilske, B.; Bai, M.; Lindenstruth, B.; Bach, M.; Rezaie, Z.; Frede, H. G.; Breuer, L. Biodegradability of a polyacrylate superabsorbent in agricultural soil. *Environ. Sci. Pollut Res. Int.* **2014**, *21* (16), 9453−9460.

(20) Ma, X. J.; Xia, H. L. Treatment of water-based printing ink wastewater by Fenton process combined with coagulation. *J. Hazard. Mater.* **2009**, *162* (1), 386−390.

(21) Kumar, S.; Shayoraj, S.; Devi, N.; Dubey, S. K.; Kumar, A.; Kumar, S.; Gulati, K. Preparation, Characterization and Properties of

some Acrylic Base Latex: A Review. *Orient. J. Chem.* **2021**, *37* (5), 1002−1016.

(22) Shao, T.; Gong, Y.; Chen, X.; Chen, L. Preparation and properties of novel self-crosslinking long fluorocarbon acrylate (MMA-BA-DFMA-HPMA) polymer latex with mixed surfactants. *Chem. Zvesti* **2021**, *75* (10), 5561−5569.

(23) Lyu, B.; Li, X.; Liu, H.; Gao, D.; Ma, J.; Zhang, M. Preparation of an amphiphilic Janus SiO2/fluorinated polyacrylate latex film and its application as a hydrophobic fabric agent. *J. Colloid Interface Sci.* **2021**, *599*, 88−99.

(24) Yang, Y.; Chen, J.; Ma, G.; Yang, D. Waterborne Cross-Linkable Polyacrylate Latex Coatings with Good Water Resistance and Strength Stabilized by Modified Hectorite. *Polymers (Basel)* **2021**, *13* (15), 2470.

(25) Gunnewiek, R. F. K.; Mendes, C. F.; Kiminami, R. H. G. A. Synthesis of Cr2O3 nanoparticles via thermal decomposition of polyacrylate/chromium complex. *Mater. Lett.* **2014**, *129*, 54−56.

(26) Li, J.; Xu, H.; Shi, J.; Li, C.; Bao, C. Studies of the major degradation products of a higher alkyl polyacrylate using pyrolysis gas chromatography-mass spectrometry. *Anal. Chim. Acta* **1999**, *402* (1−2), 311−318.

(27) Sun, Y.; Gu, Y.; Zhang, H.; Zhang, X. Adsorption properties of macroporous exchangers functionalized with various weak-base groups for aromatic acids: Coupling DFT simulation with batch experiments. *J. Environ. Chem. Eng.* **2021**, *9* (5), 106026.

(28) Boyer, T. H.; Fang, Y.; Ellis, A.; Dietz, R.; Choi, Y. J.; Schaefer, C. E.; Higgins, C. P.; Strathmann, T. J. Anion exchange resin removal of per- and polyfluoroalkyl substances (PFAS) from impacted water: A critical review. *Water Res.* **2021**, *200*, 117244.

(29) Gao, P.; Chen, D.; Chen, W.; Sun, J.; Wang, G.; Zhou, L. Facile synthesis of amine-crosslinked starch as an efficient biosorbent for adsorptive removal of anionic organic pollutants from water. *Int. J. Biol. Macromol.* **2021**, *191*, 1240−1248.

(30) Zeng, S.; Long, J.; Sun, J.; Wang, G.; Zhou, L. A review on peach gum polysaccharide: Hydrolysis, structure, properties and applications. *Carbohydr. Polym.* **2022**, *279*, 119015.

(31) Song, Y.; Tan, J.; Wang, G.; Zhou, L. Superior amine-rich gel adsorbent from peach gum polysaccharide for highly efficient removal of anionic dyes. *Carbohydr. Polym.* **2018**, *199*, 178−185.

(32) Lu, Z.; Bajwa, B. S.; Otome, O. E.; Hammond, G. B.; Xu, B. Multifaceted Ion Exchange Resin-Supported Hydrogen Fluoride: A Path to Flow Hydrofluorination. *Green Chem.* **2019**, *21* (9), 2224−2228.

(33) Galletti, A. M. R.; Antonetti, C.; De Luise, V.; Martinelli, M. A sustainable process for the production of γ-valerolactone by hydrogenation of biomass-derived levulinic acid. *Green Chem.* **2012**, *14* (3), 688−694.

(34) Duclos, L.; Chattot, R.; Dubau, L.; Thivel, P.-X.; Mandil, G.; Laforest, V.; Bolloli, M.; Vincent, R.; Svecova, L. Closing the loop: life cycle assessment and optimization of a PEMFC platinum-based catalyst recycling process. *Green Chem.* **2020**, *22* (6), 1919−1933.

(35) Mahata, B. K.; Chung, K.-L.; Chang, S.-m. Removal of ammonium nitrogen (NH4+-N) by Cu-loaded amino-functionalized adsorbents. *Chem. Eng. J.* **2021**, *411*, 128589.

(36) Verma, R.; Sarkar, S. Trace Cr (VI) Removal: Evidence of Redox-Active Ion Exchange by a Weak-Base Anion Exchanger. *Ind. Eng. Chem. Res.* **2020**, *59* (48), 21187−21195.

(37) Peters, A.; Hönen, P.; Overbeek, A.; Griffioen, S.; Annable, T. A new generation of water-borne ink binders for packaging films and paper (Part II). *Serf Coat. Int. Pt B-C* **2001**, *84* (4), 249−253.

(38) Bao, Y.; Ma, J.; Zhang, X.; Shi, C. Recent advances in the modification of polyacrylate latexes. *J. Mater. Sci.* **2015**, *50* (21), 6839−6863.

(39) Parvate, S.; Mahanwar, P. Advances in self-crosslinking of acrylic emulsion: what we know and what we would like to know. *J. Dispers Sci. Technol.* **2019**, *40* (4), 519−536.

(40) Luo, X.; Yuan, J.; Liu, Y.; Liu, C.; Zhu, X.; Dai, X.; Ma, Z.; Wang, F. Improved Solid-Phase Synthesis of Phosphorylated Cellulose Microsphere Adsorbents for Highly Effective Pb2+ Removal

from Water: Batch and Fixed-Bed Column Performance and Adsorption Mechanism. *ACS Sustain. Chem. Eng.* **2017**, *5* (6), 5108−5117.

(41) Trublet, M.; Scukins, E.; Carabante, I.; Rusanova, D. Competitive Sorption of Metal Ions on Titanium Phosphate Sorbent (TiP1) in Fixed-Bed Columns: A Closed-Mine Waters Study. *ACS Sustain. Chem. Eng.* **2019**, *7* (9), 8145−8154.

(42) Arshadi, M.; Abdolmaleki, M. K.; Eskandarloo, H.; Azizi, M.; Abbaspourrad, A. Synthesis of Highly Monodispersed, Stable, and Spherical NZVI of 20−30 nm on Filter Paper for the Removal of Phosphate from Wastewater: Batch and Column Study. *ACS Sustain. Chem. Eng.* **2018**, *6* (9), 11662−11676.

(43) Xia, K.; Liu, X.; Chen, Z.; Fang, L.; Du, H.; Zhang, X. Efficient and sustainable treatment of anionic dye wastewaters using porous cationic diatomite. *J. Taiwan Inst Chem. Eng.* **2020**, *113*, 8−15.

(44) Galvis-Sánchez, A. C.; Sousa, A. M. M.; Hilliou, L.; Gonçalves, M. P.; Souza, H. K. S. Thermo-compression molding of chitosan with a deep eutectic mixture for biofilms development. *Green Chem.* **2016**, *18* (6), 1571−1580.

(45) Hashemi, H.; Bahrami, S.; Emadi, Z.; Shariatipor, H.; Nozari, M. Optimization of ammonium adsorption from landfill leachate using montmorillonite/hematite nanocomposite: response surface method based on central composite design. *Desalination Water Treat.* **2021**, *232*, 39−54.

(46) Al-Muntasheri, G. A.; Nasr-El-Din, H. A.; Peters, J. A.; Zitha, P. L. J. Thermal decomposition and hydrolysis of polyacrylamide-co-tert-butyl acrylate. *Eur. Polym. J.* **2008**, *44* (4), 1225−1237.

(47) Peng, L.; Zhou, S.; Wang, X.; Zhao, M.; Chen, D.; Tie, J. Adsorption of reactive green 19 from water using polyaniline/bentonite. *J. Water Reuse Desalination* **2016**, *6* (4), 515−523.

(48) Sun, D.; Zhang, X.; Wu, Y.; Liu, X. Adsorption of anionic dyes from aqueous solution on fly ash. *J. Hazard. Mater.* **2010**, *181* (1−3), 335−342.

(49) Gong, J.-L.; Zhang, Y.-L.; Jiang, Y.; Zeng, G.-M.; Cui, Z.-H.; Liu, K.; Deng, C.-H.; Niu, Q.-Y.; Deng, J.-H.; Huan, S.-Y. Continuous adsorption of Pb (II) and methylene blue by engineered graphite oxide coated sand in fixed-bed column. *Appl. Surf. Sci.* **2015**, *330*, 148−157.

(50) García-Mateos, F. J.; Ruiz-Rosas, R.; Marqués, M. D.; Cotoruelo, L. M.; Rodríguez-Mirasol, J.; Cordero, T. Removal of paracetamol on biomass-derived activated carbon: Modeling the fixed bed breakthrough curves using batch adsorption experiments. *Chem. Eng. J.* **2015**, *279*, 18−30.

(51) Haque, E.; Lo, V.; Minett, A. I.; Harris, A. T.; Church, T. L. Dichotomous adsorption behaviour of dyes on an amino-functionalised metal-organic framework, amino-MIL-101(Al). *J. Mater. Chem. A* **2014**, *2* (1), 193−203.

(52) Yang, D.; Liu, C.; Quan, P.; Fang, L. Molecular mechanism of high capacity-high release transdermal drug delivery patch with carboxyl acrylate polymer: Roles of ion-ion repulsion and hydrogen bond. *Int. J. Pharm.* **2020**, *585*, 119376.

(53) Ip, A. W. M.; Barford, J. P.; McKay, G. A comparative study on the kinetics and mechanisms of removal of Reactive Black 5 by adsorption onto activated carbons and bone char. *Chem. Eng. J.* **2010**, *157* (2−3), 434−442.

(54) Banaei, A.; Farokhi Yaychi, M.; Karimi, S.; Vojoudi, H.; Namazi, H.; Badiei, A.; Pourbasheer, E. 2,2'-(butane-1,4-diylbis (oxy))dibenzaldehyde cross-linked magnetic chitosan nanoparticles as a new adsorbent for the removal of reactive red 239 from aqueous solutions. *Mater. Chem. Phys.* **2018**, *212*, 1−11.